

Cite this: *J. Mater. Chem. A*, 2018, 6, 20844

Light-driven carbon dioxide reduction coupled with conversion of acetylenic group to ketone by a functional Janus catalyst based on keplerate $\{\text{Mo}_{132}\}^\dagger$

Joyeeta Lodh,^{ab} Apabrita Mallick^{ab} and Soumyajit Roy ^{*ab}

Catalysts enabling CO₂ reduction coupled with another organic reaction are rare. In this study, we report such a catalyst keplerate $\{\text{Mo}_{132}\}$, which catalyses photochemical carbon dioxide reduction to formic acid coupled with organic transformation, *i.e.*, hydration of phenylacetylene to acetophenone in visible light. It initially oxidizes water and injects the reducing equivalents for reduction of carbon dioxide at the same time, converting acetylenic group to ketone. Our designed redox Janus catalyst provides an inexpensive pathway to achieve carbon dioxide reduction as well as conversion of phenylacetylene to acetophenone, which is an industrially important precursor.

Received 29th June 2018
Accepted 30th September 2018

DOI: 10.1039/c8ta06243a

rsc.li/materials-a

Introduction

An increase in energy demand and greenhouse gas emission has called for a need to reduce carbon dioxide¹ chemically, which has been achieved in this study using polyoxometalate $\{\text{Mo}_{132}\}$.^{2–5} It can become an indispensable key technology to address the global energy and environmental crisis.⁶ As light is abundant, it can be harnessed⁷ to replace the existing use of fossil fuel reserve if it can valorize CO₂. CO₂ valorization can be achieved by its direct reduction^{8–12} alternatively as a coupled process, where a sacrificial oxidizing agent^{13,14} is required. In our laboratory, we have developed pathways for reduction of CO₂ coupled with oxidation of water^{15,16} using heterogenized soft-oxometalates.^{17–20} Here, we take the next step and employ a dual-functional catalyst, a Janus catalyst, synthesized and characterized first by the Müller group of Germany,^{2–5} which can reduce CO₂ and convert the acetylenic moiety to ketone. Before we describe the modus operandi and the design of our catalyst in detail, we review the literature on CO₂ reduction to put our study in perspective.

The field of CO₂ reduction has been gaining attention for quite a while²¹ owing to the prospect of reduction of greenhouse gases and also for the option to generate high-energy liquid fuels, such as CH₃OH^{22,23} and HCOOH,^{16,17} and even higher carbon containing congeners²⁴ including various fine

chemicals. Lehn and Sauvage, in 1982 and 1986, conducted path-breaking studies in the field of carbon dioxide reduction using metal-porphyrins,²⁵ Ni-cyclams²⁶ and polyporphyrins. Ishitani has reported visible light photocatalytic CO₂ reduction for both carbon nitride nanosheets²⁷ and ytterbium–tantalum²⁸ oxynitride coupled with a binuclear Ru(II) complex. Furthermore, CuGaO₂, which is a p-type semi-conductor coupled with Ru(II)–Re(I) supramolecular catalyst to reduce CO₂ to CO photoelectrochemically, has also been reported.²⁹ Yaghi and co-workers have pioneered the field of electrocatalytic CO₂ reduction using porphyrin-containing active sites of covalent organic frameworks.³⁰ They have also pioneered plasmon-enhanced photocatalytic CO₂ reduction under visible light using metal organic framework-coated nanoparticles, Ag/Re₃-MOF.³¹ Frei's group has conducted notable research on photoinduced CO₂ reduction using Cd and CdSe nanoparticles. Abe *et al.* have led the efforts on photoreduction of CO₂ to formate using a Cd–Zn alloy catalyst.³²

In our recent studies, we have approached CO₂ reduction from the perspective of a coupling reaction with water oxidation, where soft-oxometalates (SOMs) have been used as photoactive and photosensitizing components. The constituents of all these SOMs are oxometalates with photo-excitable M=O units. Here, we take the next step and employ a molecular (NH₄)₄₂[Mo^{VI}₇₂Mo^V₆₀O₃₇₂(CH₃COOH)₃₀(H₂O)₇₂]·hydrate $\{\text{Mo}_{132}\}$ **1** as a Janus catalyst and photoexcite it first using visible light in the presence of Ru(II)(bpy)₃Cl₂ to oxidise water. The Janus function of the catalyst now comes into play. It catalyzes the reduction of CO₂ to formic acid by injecting the generated electrons and protons. Concomitantly, it can switch to an organic reaction by the generated protons in the medium along with oxygen and water. Hence, here, we choose to couple CO₂

^aEFAML, College of Chemistry, Central China Normal University, 152 Luoyu Road, Wuhan, P. R. China. E-mail: s.roy@mail.ccnu.edu.cn

^bEFAML, Materials Science Centre, Department of Chemical Sciences, Indian Institute of Science Education & Research, Mohanpur Campus, Kolkata, India. E-mail: s.roy@iiserkol.ac.in

† Electronic supplementary information (ESI) available. See DOI: 10.1039/c8ta06243a

reduction with the hydration of an acetylenic bond to synthesize a ketone. More specifically, we hydrolyze phenylacetylene to acetophenone simultaneously while reducing CO₂ to formic acid. It might be noted here that organic precursors such as acetophenone in particular are vital for pharmaceutical industries³³ for the synthesis of drugs, including pyrrobutamine,³⁴ dextropropoxyphene,³⁵ trihexyphenidyl,³⁶ pyridinol,³⁷ and aspaminol.³⁸ Even though the synthesis of such a vital precursor has been made relatively cheaper, yet, the challenge is to economize an efficient *modus operandi* for the synthesis of this precursor. Organic transformation in the presence of visible light^{39–41} coupled with CO₂ reduction is a way forward in that direction. The reaction is important in the present context as it is carried out under a mild reaction condition⁴² as well as atom economically⁴³ along with a thermodynamically uphill reaction⁴⁴ such as that of CO₂ reduction.

We now describe the structure of the catalyst in detail.^{15–18} The Janus catalyst is (NH₄)₄₂[Mo₇₂^{VI}Mo₆₀^VO₃₇₂(CH₃COOH)₃₀·(H₂O)₇₂]·ca. 300H₂O.^{4,45} The molecule has an icosahedral point group and consists of 12 [(Mo^{VI})(Mo^{VI})₅]⁴⁶ pentagons disposed at the vertices of the icosahedron. Here, the central pentagonal unit is pentagonal bipyramidal [MoO₇], which is linked *via* O bridging atoms to 5 [MoO₅(H₂O)] octahedra. We believe that the coordinated water molecules in these octahedral sites act as active sites for the hydration of acetylenic groups. Moreover, there are 30 [Mo₂^V] linkers, each of which connects two [MoO₅(H₂O)] of two different [(Mo^{VI})(Mo^{VI})₅] units forming the icosahedral cluster. The mixed valent Mo^V/Mo^{VI} centres act as the redox centres of the catalyst in the catalytic process, and such abundance of mixed valent centres led us to choose this catalyst for the redox reaction. It may be mentioned that in recent times, various groups have been involved in exploiting the alkyne chemistry to generate viable industrially important chemicals. Recent research includes hydration of alkynes using systems involving Au salts^{47–49} and ruthenium-^{50,51} and platinum-based catalysts.⁵² Here, we have taken the next step; we have coupled alkyne hydroxylation with CO₂ reduction. Now, we describe our experimental design and results.

Experimental procedure

Materials and reagents

All the materials used for the experiments are available commercially and have not been purified further. The glass apparatus used was first washed in acid bath, followed by water and finally, it was rinsed with water. All the experiments were carried out in doubly distilled deionized water.

Synthesis of (NH₄)₄₂[Mo₇₂^{VI}Mo₆₀^VO₃₇₂(CH₃COOH)₃₀(H₂O)₇₂]·hydrate (1)

To a solution of (NH₄)₆Mo₇O₂₄·4H₂O (5.6 g, 4.5 mmol) and CH₃COONH₄ (12.5 g, 162.2 mmol) in H₂O (250 mL), N₂H₆·SO₄ (0.8 g, 6.1 mmol) was added and stirred for 10 min. The color was observed to change from blue to green. Then, 50% (v/v) CH₃COOH (83 mL) was added. The green solution was stored at 22 °C in an open vessel without further stirring. The color

slowly turned brown. The precipitated red brown crystals obtained after 3–4 days were filtered off through a glass frit, washed with 90% ethanol and diethyl ether and dried in air. Yield: 3.3 g (52% based on Mo).

Synthesis of Ru(bpy)₃Cl₂

Reagent grade dimethyl formamide (7 mL) was refluxed with 2,2-bipyridine (1.195 g, 7.649 mmol), LiCl (1.077 g) and RuCl₃·3H₂O (1 g, 8.824 mmol) for 8 hours. Reagent grade acetone (32 mL) was added to the reaction mixture as it cooled down to room temperature. The reaction mixture was kept overnight at 0 °C. The solution was then filtered, and black crystalline substance was obtained. The crystals were washed thrice with water and then with diethyl ether and dried by suction.

General reaction procedure for photocatalytic CO₂ reduction

The photocatalytic carbon dioxide reduction was conducted as follows: desired amounts (0.1–0.8 μmol) of {Mo₁₃₂}, *i.e.*, our catalyst and Ru(bpy)₃Cl₂ (0.2 μmol) were taken in 10 mL of degassed double distilled water. Furthermore, the reaction mixture was purged with CO₂ gas for 2 hours in a sealed reaction vial. The reaction mixture was kept in blue LED light and monitored at different time intervals (2–24 hours). A 20 μL aliquot of the reaction mixture was taken out and further diluted with 10 mL of doubly distilled water for monitoring the products with GC-MS. The presence of formic acid was also detected using GC-MS. All the quantifications of formic acid were performed using GC-MS.

General procedure for coupling photocatalytic CO₂ reduction with organic hydroxylation reactions

The reaction was conducted photochemically in a 10 mL quartz tube with phenylacetylene (2 mmol), HCl (12 N, 10 μL), water, [Mo₁₃₂] catalyst (0.1–0.8 μmol) and Ru(bpy)₃Cl₂ (2 mg) kept under blue LED light. The reaction mixture was sealed in a reaction vial, and CO₂ was purged for 2 hours. The light flux was measured to be 0.32 W cm⁻² (at 475 nm). The reaction was monitored with thin layer chromatography at different time intervals and eventually, the product acetophenone was quantified using GC-MS.

Characterisation technique

Raman spectroscopy. Raman spectroscopy (Horiba Jobin Yvon LABRAM HR800) was employed using a He–Ne ion laser of wavelength 633 nm as the excitation source to analyse the catalyst before and after the course of the reaction.

¹H NMR spectroscopy. ¹H NMR of the isolated products was recorded on a Jeol 400 MHz Spectrometer.

Gas chromatography-mass spectrometry (GC-MS). The products were identified and analyzed using Trace 1300 GC and ISQ qd single quadrupole mass spectrometer with a TG-5MS capillary column (30 m × 0.32 mm × 0.25 μm) supplied by Thermo Fisher Scientific, India.

Fourier-transform infra-red (FT-IR) spectroscopy. The FT-IR spectra were collected using a PerkinElmer Spectrum RX1

spectrophotometer. The sample was grounded with KBr and was recorded within the range of 2000–450 cm^{-1} .

Results and discussions

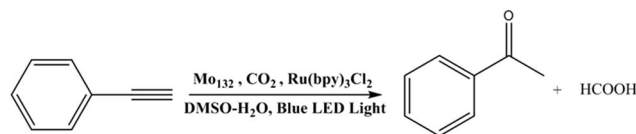
About the Janus catalyst

$(\text{NH}_4)_{42}[\text{Mo}_{72}^{\text{VI}}\text{Mo}_{60}^{\text{V}}\text{O}_{372}(\text{CH}_3\text{COOH})_{30}(\text{H}_2\text{O})_{72}] \cdot \text{ca. } 300\text{H}_2\text{O}$ (1)

The polyoxometalate **1** (Fig. 1) serves as an active catalyst for photochemical carbon dioxide reduction coupled with organic transformation of phenylacetylene to acetophenone in water. It is a keplerate⁵³ anion having a diameter of 2.9 nm. The spherical cluster consists of 132 molybdenum centres out of which 72 are Mo^{VI} , and the rest 60 are Mo^{V} . The purity of the synthesized $\{\text{Mo}_{132}\}$ was confirmed using FT-IR spectra. The FT-IR spectra of $\{\text{Mo}_{132}\}$ in the region of 2000–450 cm^{-1} are shown in Fig. S6.† The characteristic bands for $\{\text{Mo}_{132}\}$ were found at 968 and 935, 792 and 724 cm^{-1} due to the presence of $\text{Mo}=\text{O}$ bond and $\text{Mo}-\text{O}-\text{Mo}$ bond. The peaks at 1546 and 1404 cm^{-1} denoted the presence of COO^- and NH_4^+ groups, respectively (Fig. S6†). Both the redox activity and photoactivity of the Mo centres in the cluster facilitated the reaction. We believe that this active species is responsible for photocatalytic CO_2 reduction coupled with hydration of phenylacetylene.

Photocatalytic carbon dioxide reduction

The photochemical carbon dioxide reduction was performed using catalyst **1** under nitrogen atmosphere. On purging CO_2 , it gets linked with the Mo_2 unit of the catalyst and thus creates a CO_2 -adsorbed species $\{\text{Mo}_{132}-\text{CO}_2\}$.⁵⁴ $\text{Ru}(\text{bpy})_3\text{Cl}_2$ has been used as a photosensitizer (PS). On photo-excitation using blue LED, $\text{Ru}(\text{bpy})_3^{2+}$ transfers its energy to CO_2 -adsorbed catalyst species, forming $\{\text{Mo}_{132}-\text{CO}_2\}^*$.^{55–58} The water in the reaction medium acts as a sacrificial electron donor to reduce Mo^{VI} centres in excited catalyst species to Mo^{V} , thus forming $\{\text{Mo}_{132}-\text{CO}_2\}^-$.⁵⁹ This facilitates the reduction of adsorbed carbon dioxide to formic acid. In the absence of $\text{Ru}(\text{bpy})_3\text{Cl}_2$, formic acid or acetophenone is not detected in the visible light, indicating the fact that catalytic cycle is initiated by the photosensitizer. The concentration of $\{\text{Mo}_{132}\}$ is kept constant and that of $\text{Ru}(\text{bpy})_3\text{Cl}_2$ is varied; the activity of the catalyst then increases. However, when the concentration of $\text{Ru}(\text{bpy})_3\text{Cl}_2$ is further



Scheme 1 Schematic representation of the coupling process using $\{\text{Mo}_{132}\}$ as the catalyst under blue LED light in the presence of $\text{Ru}(\text{bpy})_3\text{Cl}_2$ as a photosensitizer.

increased, the activity remains unchanged. The optimised ratio for maximum activity is achieved with 1 : 1 mole ratio. The reduction yields formic acid selectively from carbon dioxide, and the same is detected through cyclic voltammetry (CV) and gas chromatography MS (GC-MS). We could not trace the presence of any other liquid or gaseous products other than formic acid. The peak corresponding to the reduction of carbon dioxide at around -0.6 V from the CV experiments *vs.* the Ag/AgCl electrode denotes the conversion of CO_2 to HCOOH (Fig. S5†). The formic acid formed is quantified by GC-MS. The isotopic $^{13}\text{CO}_2$ is used instead of $^{12}\text{CO}_2$ in the photocatalytic reaction. The products are characterized using gas chromatography-mass spectrometry (Fig. S7†). After the catalysis, the peak appearing at 1.7 min with $m/z = 75$ corresponds to ethyl formate formed after esterification of formic acid found in the medium with ethanol. This validates the fact that formic acid is derived from $^{13}\text{CO}_2$. The simultaneously occurring water oxidation yields oxygen in the reaction medium, which is detected using a YSI Clark-type electrode (Fig. S1 and S2†). This is further confirmed from CV experiments. A sharp increase in current is observed at 1.2 V *vs.* Ag/AgCl electrode, which is a characteristic of water oxidation (Fig. S5†). We have later investigated the effects of catalyst loading, pH and reaction time on the yield of the reactions depicted in Scheme 1.

Coupling organic transformation with CO_2 reduction

A more detailed picture leads us to propose a pathway for this reaction (Fig. 2). On purging CO_2 in the reaction medium, peaks have been observed followed by increase in the current in the cyclic voltammogram. The peaks correspond to the adsorption of CO_2 on the surface of the catalyst, resulting in the formation of CO_2 -adsorbed catalyst species (Fig. 2b). As discussed previously, while the electrons generated from water oxidation are utilized for carbon dioxide reaction, the generated protons are taken up by organic substrates for their oxidation. In this study, we have used phenylacetylene as the organic moiety. The triple bonds in phenylacetylene accept the proton and the alkyne functionality is hydrogenated to form a vinylic carbocation. Once the proton is bound, the carbocation formed gets attacked by the water molecules in the reaction medium, and the loss of proton gives the addition product acetophenone. To probe the pathway, we have performed the reaction by replacing H_2O with D_2O ; from the NMR spectra (Fig. 2a), a peak is observed at 3.06 ppm, which corresponds to the D substitution in the terminal methyl group.

To investigate the dependency of the coupling process of organic transformation and photochemical carbon dioxide

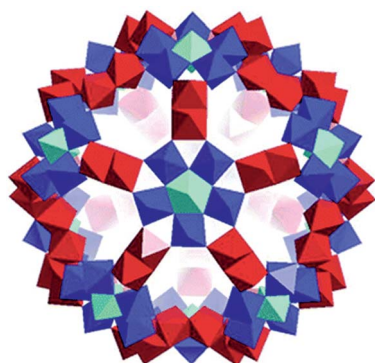


Fig. 1 Structure of the catalyst $\{\text{Mo}_{132}\}$.

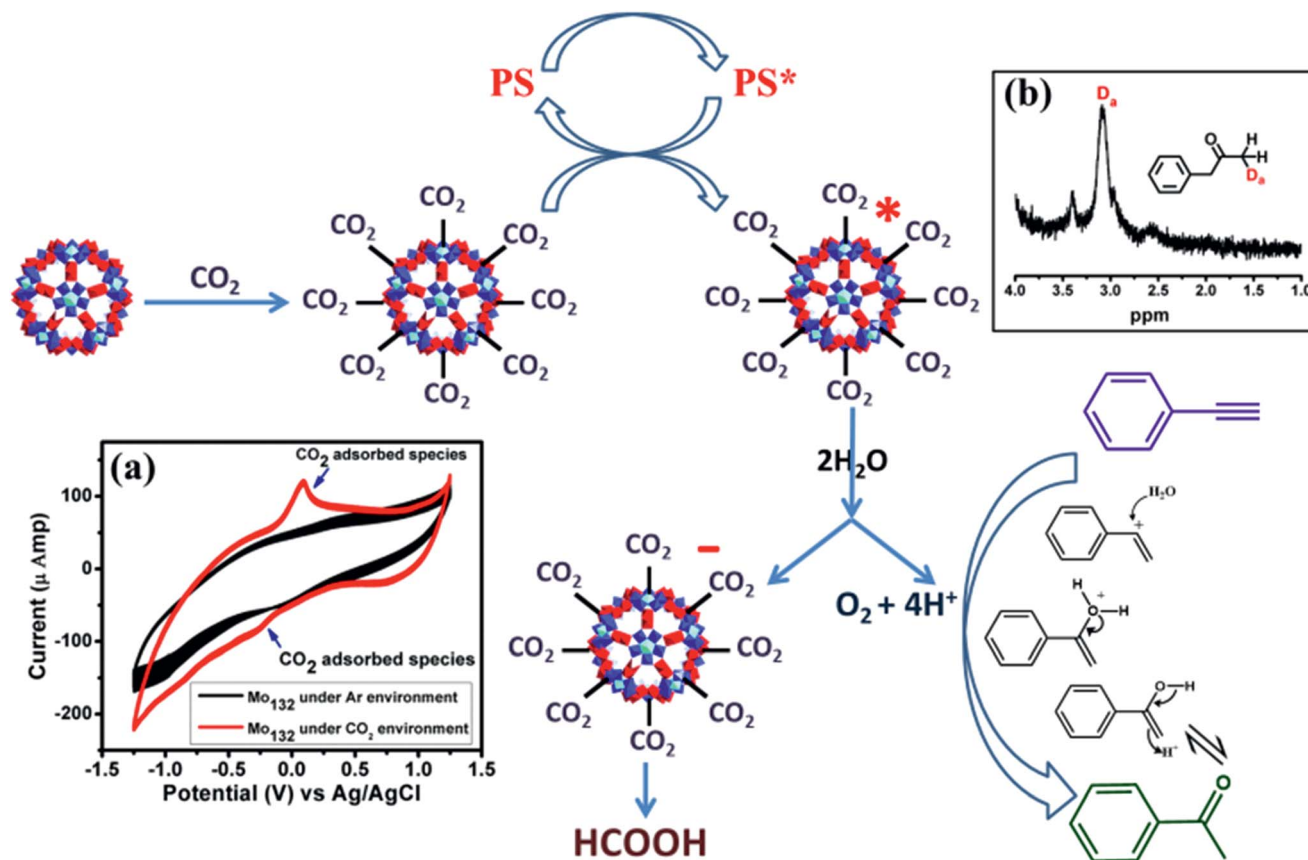


Fig. 2 A probable pathway for photocatalytic carbon dioxide reduction and organic reaction using {Mo₁₃₂} as a catalyst. (a) Cyclic voltammogram of the reaction mixture showing CO₂-adsorbed species (b) ¹H NMR showing deuterium substitution in the product obtained from the reaction mixture in D₂O.

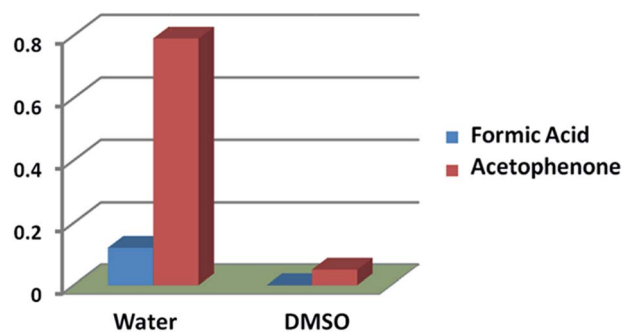


Fig. 3 Plots representing yields of formic acid and acetophenone in reaction media of water and DMSO.

reduction, we performed the reaction in different kinds of solvents, such as dry DMF and dry DMSO, keeping the other conditions constant. In these aprotic solvents, hardly any trace of formic acid was found. We believe that the trace amount of water present along with DMF or DMSO led to the formation of acetophenone. DMSO/water (1 : 1) gave the optimum yield of the reaction with 0.12 mmol of formic acid and 0.79 mmol of acetophenone (Fig. 3). DMSO does not play any role other than solubilising the organic substrate and providing the reaction

with ROS. The same reaction was also performed in the absence of light to show the effect of light on the reaction. No products were obtained under this condition, and this implied the fact that the reaction was dependent on light. Thus, water and light are integral parts of our reaction. A slight excess acid is needed to ensure optimum transformation of organic substrates. In the absence of an acid, phenylacetylene tends to polymerise. The biphasic solvent systems such as DMSO/H₂O allow easy separation of the catalyst from the products.

Effect of pH on the reaction

Now, we investigate the effect of pH on the reaction system. It is a known fact that carbon dioxide reduction is facilitated by decrease in pH, whereas water oxidation is characterised by an increase in pH. This could be well understood by taking into account these two reaction equilibria:



The carbon dioxide reduction is a proton coupled process; the reduced product is facilitated by increasing proton concentration, *i.e.*, with decrease in pH. The water oxidation

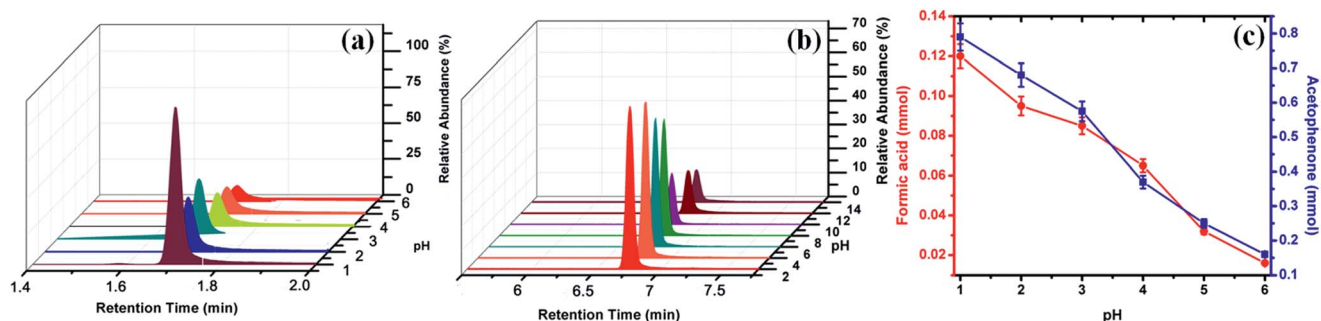


Fig. 4 GC-MS plots of (a) formic acid and (b) acetophenone obtained at various pH. (c) Plot showing yield of formic acid and acetophenone at different pH.

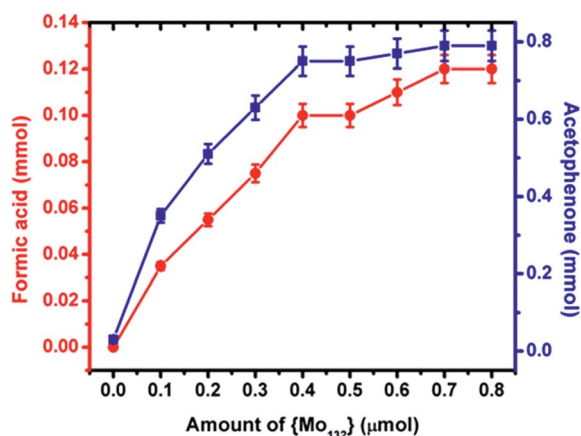


Fig. 5 Plot showing yield of formic acid and acetophenone for various loading of $\{Mo_{132}\}$ catalyst.

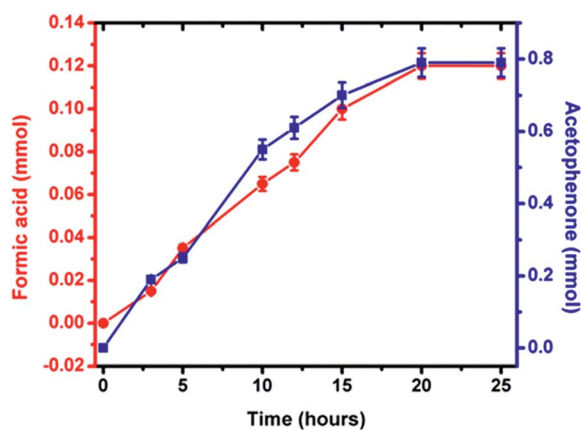


Fig. 6 Plots showing yields of formic acid and acetophenone at different time intervals.

releases protons into the reaction medium and thus, an increase in pH facilitates water oxidation. The addition of a proton to the carbon with more number of hydrogen (terminal carbon atom) suggests the fact that it is a Markovnikov addition. The Markovnikov additions of hydrogen over terminal alkynes result in methyl ketone. The electrons in the triple

bonds of the terminal alkynes act as Lewis bases and thus attack the protons released during water oxidation. This protonates the carbon with the most number of hydrogen substituents. Thus, hydration of terminal alkynes could also be stated as a proton coupled process, wherein the formation of methyl ketone is favoured by increasing proton concentration in the reaction medium. Thus, considering the overall mechanism, the reaction is facilitated by decreasing pH. The maximum yield of formic acid was observed to be 0.12 mmol at pH 1, whereas that of acetophenone was 0.79 mmol (Fig. 4).

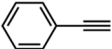
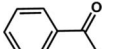
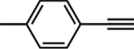
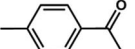
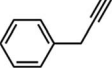
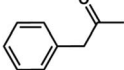
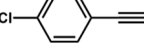
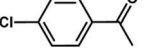
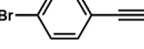
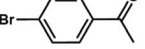
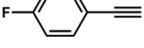
Effect of catalyst loading on the reaction

The amount of product formation varied with the amount of catalyst following the kinetics of heterogeneous catalytic reaction. The concentration of products was found to increase with the increase in the amount of catalyst only up to a certain limit, *i.e.*, 0.4 μmol of catalyst **1** (Fig. 5). However, with further increase in the concentration of catalyst, the concentration of products becomes almost constant. This is because of the fact that the reaction is dependent on the active surface area of the catalyst, which becomes constant after a certain amount of catalyst loading. The maximum turnover number (TON) of CO_2 reduction reaction is 300 with respect to per mole of catalyst **1**, whereas that of hydration of phenylacetylene is found to be 1975.

Effect of time on the reaction

Next, we performed time-dependent experiments at pH 1 with 0.4 μmol of catalyst **1**. The amount of formic acid is found to increase with increasing time (Fig. 6). The nature of the plot indicating the formation of products with time is near-sigmoidal, which implies possibility of operation of heterogeneous catalysis in the reaction. Owing to the overlapping nature of near-linear and near-sigmoidal nature of the plot, we envisage molecular and heterogeneous catalysis to be the mode of catalysis. Both the reactions have an initial lag phase of few hours (Fig. 6), which might be the time necessary for the activation of the catalyst. The reaction required *ca.* 24 hours for completion. The maximum turnover frequencies (TOF) for HCOOH and acetophenone at the end of 24 hours of reaction are 12.5 h^{-1} and 82.29 h^{-1} , respectively.

Table 1 Effects of different substitutions of phenylacetylene on reaction yield

Reagent	Product	Yield
		79
		83
		86
		91
		8
		7
	No reaction	—

Effect of the substrate

The effect of substitutions on the substrates in hydration of phenylacetylene to acetophenone could be correlated with the stability of the carbonium ion formed during the rate determining step. Solvation plays a significant role in the carbonium ions derived from the alkynes and hence, steric hindrance in such solvation can have a greater impact. As mentioned previously, substitution greatly alters the reaction rates (Table 1). It has been observed that *para*-substituted phenylacetylene undergoes a reaction faster than phenylacetylene itself. This observation indicates that the presence of electron donating groups accelerates the reaction, whereas electron withdrawing groups at the *para* position decrease the rate of reaction. Furthermore, for some substituted products, such as trifluoromethyl-substituted phenylacetylene and

trimethyl(phenylethynyl)silane, no reactivity was observed owing to their electron deficiency and volatility, respectively. This observation further indicates that the reaction proceeds *via* cation formation. We also observe that the stability of the intermediate cation plays a predominant role in the product formation. The reactivity of internal alkynes has been found to be lower, whereas the use of terminal alkynes as substrates and 0.4 μmol loading of catalyst **1** led to conversions ranging from 79% to 91%. The rate determining step of the organic transformation was marked by the formation of carbonium ion, which further reacted with water in the medium and tautomerized to form ketone. This was proved by performing the reaction with D_2O .

Stability of the catalyst

We further investigated the stability of the catalyst using Raman spectroscopy (Fig. 7) before and after the reaction. Raman spectra of the catalyst were found to be identical in both the cases. This result highlighted the fact that the cluster remains intact during the course of the reaction. To confirm the recyclability of the catalyst, we have used catalyst **1** up to 10 catalytic cycles. The catalyst has been found to remain intact even after 10 cycles, and the yields of the reduction products, *i.e.*, formic acid and acetophenone remain almost the same. Hence, we report a stable catalyst, which could be used to catalyse the reaction under photocatalytic conditions.

Conclusions

To summarize, herein, we report a simple, effective and green route to photochemically reduce carbon dioxide to formic acid and couple it with an organic reaction to produce ketones from corresponding alkyne substrates. We have used keplerate polyoxometalate – $\{\text{Mo}_{132}\}$ and exploited its photocatalytic activity to carry out the above reactions as a dual-functional Janus catalyst. We found that the redox activity of $\text{Mo}^{\text{V}}/\text{Mo}^{\text{VI}}$ centre of the catalyst drives the whole coupling process. This is important

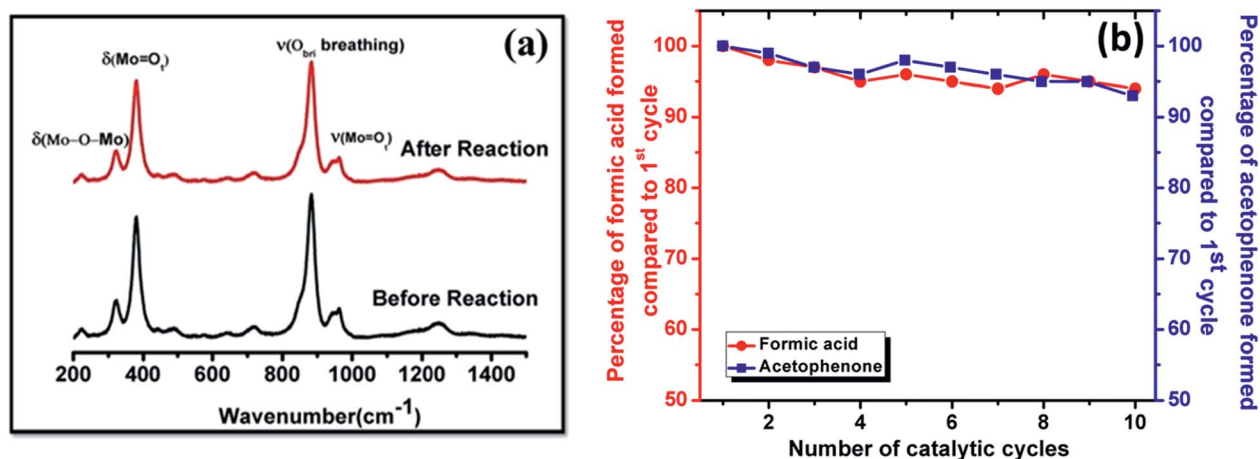


Fig. 7 (a) Raman spectra of $\{\text{Mo}_{132}\}$ before and after reaction showing identical peaks. (b) Recyclability of $\{\text{Mo}_{132}\}$ in photochemical CO_2 reduction and organic hydroxylation.

from the perspective of synthetic chemistry as well as green chemistry as the Janus catalyst used here is inexpensive, efficient and environmentally friendly. It is also one of the first examples of how a Janus catalyst can be used in organic transformations coupled with carbon dioxide reduction. This study can further open up new avenues in the area of catalysis in the context of CO₂ valorization chemistry and organic syntheses.

Conflicts of interest

There are no conflicts to declare.

Acknowledgements

SR gratefully acknowledges the start-up and FIRE grants from IISER-Kolkata. The financial support from CCNU, China and NSFC is gratefully acknowledged.

References

- S. Chakravarty, A. Chikkatur, H. De Coninck, S. Pacala, R. Socolow and M. Tavoni, *Proc. Natl. Acad. Sci. U. S. A.*, 2009, **106**, 11884–11888.
- S. Garai, H. Bögge, A. Merca, O. A. Petina, A. Grego, P. Gouzerh, E. T. Haupt, I. A. Weinstock and A. Müller, *Angew. Chem., Int. Ed.*, 2016, **55**, 6634–6637.
- M. Garcia-Ratés, P. Miro, A. Müller, C. Bo and J. B. Avalos, *J. Phys. Chem. C*, 2014, **118**, 5545–5555.
- A. Müller, P. Kögerler and A. Dress, *Coord. Chem. Rev.*, 2001, **222**, 193–218.
- A. Müller, E. Krickemeyer, H. Bögge, M. Schmidtman and F. Peters, *Angew. Chem., Int. Ed.*, 1998, **37**, 3359–3363.
- M. Jacobson, W. Colella and D. Golden, *Science*, 2005, **308**, 1901–1905.
- C. Y. N. Power, Bulletin of the Connecticut Academy of Science and Engineering, 2002, vol. 17, p. 1.
- C. Steinlechner and H. Junge, *Angew. Chem., Int. Ed.*, 2018, **57**, 44–45.
- C. Cometto, R. Kuriki, L. Chen, K. Maeda, T.-C. Lau, O. Ishitani and M. Robert, *J. Am. Chem. Soc.*, 2018, **140**(24), 7437–7440.
- J. Bian, Y. Qu, X. Zhang, N. Sun, D. Tang and L. Jing, *J. Mater. Chem. A*, 2018, **6**, 11838–11845.
- M. Sun, S. Yan, Y. Sun, X. Yang, Z. Guo, J. Du, D. Chen, P. Chen and H. Xing, *Dalton Trans.*, 2018, **47**, 909–915.
- Y. Fu, D. Sun, Y. Chen, R. Huang, Z. Ding, X. Fu and Z. Li, *Angew. Chem.*, 2012, **124**, 3420–3423.
- M. Pschenitzka, S. Meister and B. Rieger, *Chem. Commun.*, 2018, **54**, 3323–3326.
- S. Somasundaram, C. R. N. Chenthamarakshan, N. R. de Tacconi and K. Rajeshwar, *Int. J. Hydrogen Energy*, 2007, **32**, 4661–4669.
- S. Barman, S. Das, S. S. S. Garai, R. Pochamoni and S. Roy, *Chem. Commun.*, 2018, **54**, 2369–2372.
- S. Das, S. Kumar, S. Garai, R. Pochamoni, S. Paul and S. Roy, *ACS Appl. Mater. Interfaces*, 2017, **9**, 35086–35094.
- S. Das, S. Biswas, T. Balaraju, S. Barman, R. Pochamoni and S. Roy, *J. Mater. Chem. A*, 2016, **4**, 8875–8887.
- S. Biswas, R. Pochamoni and S. Roy, *ChemistrySelect*, 2018, **3**, 2649–2654.
- S. Roy, *CrystEngComm*, 2014, **16**, 4667–4676.
- S. Roy, *Comments Inorg. Chem.*, 2011, **32**, 113–126.
- B. Kumar, M. Llorente, J. Froehlich, T. Dang, A. Sathrum and C. P. Kubiak, *Annu. Rev. Phys. Chem.*, 2012, **63**, 541–569.
- B. Rungtaweeworanit, J. Baek, J. R. Araujo, B. S. Archanjo, K. M. Choi, O. M. Yaghi and G. A. Somorjai, *Nano Lett.*, 2016, **16**, 7645–7649.
- F. Studt, I. Sharafutdinov, F. Abild-Pedersen, C. F. Elkjær, J. S. Hummelshøj, S. Dahl, I. Chorkendorff and J. K. Nørskov, *Nat. Chem.*, 2014, **6**, 320.
- K. U. D. Calvino, A. B. Laursen, K. M. K. Yap, T. A. Goetjen, S. Hwang, B. Mejia-Sosa, A. Lubarski, K. M. Teeluck, N. Murali, E. S. Hall, E. Garfunkel, M. Greenblatt and G. C. Dismukes, *Energy Environ. Sci.*, 2018, **11**, 2550–2559.
- J. Hawecker, J.-M. Lehn and R. Ziessel, *J. Chem. Soc., Chem. Commun.*, 1984, 328–330.
- M. Beley, J.-P. Collin, R. Ruppert and J.-P. Sauvage, *J. Chem. Soc., Chem. Commun.*, 1984, 1315–1316.
- R. Kuriki, M. Yamamoto, K. Higuchi, Y. Yamamoto, M. Akatsuka, D. Lu, S. Yagi, T. Yoshida, O. Ishitani and K. Maeda, *Angew. Chem., Int. Ed.*, 2017, **56**, 4867–4871.
- K. Muraoka, H. Kumagai, M. Eguchi, O. Ishitani and K. Maeda, *Chem. Commun.*, 2016, **52**, 7886–7889.
- H. Kumagai, G. Sahara, K. Maeda, M. Higashi, R. Abe and O. Ishitani, *Chem. Sci.*, 2017, **8**, 4242–4249.
- C. S. Diercks, S. Lin, N. Kornienko, E. A. Kapustin, E. M. Nichols, C. Zhu, Y. Zhao, C. J. Chang and O. M. Yaghi, *J. Am. Chem. Soc.*, 2018, **140**, 1116–1122.
- K. M. Choi, D. Kim, B. Rungtaweeworanit, C. A. Trickett, J. T. D. Barmanbek, A. S. Alshammari, P. Yang and O. M. Yaghi, *J. Am. Chem. Soc.*, 2016, **139**, 356–362.
- G. Yin, H. Abe, R. Kodiyath, S. Ueda, N. Srinivasan, A. Yamaguchi and M. Miyauchi, *J. Mater. Chem. A*, 2017, **5**, 12113–12119.
- L. Astudillo, G. Schmeda-Hirschmann, R. Soto, C. Sandoval, C. Afonso, M. Gonzalez and A. Kijjoa, *World J. Microbiol. Biotechnol.*, 2000, **16**, 585.
- A. Casy and A. Parulkar, *Can. J. Chem.*, 1969, **47**, 423–427.
- R. W. Souter, *J. Chromatogr. A*, 1977, **134**, 187–190.
- M. Poirier, N. Curran, K. McErlane and E. Lovering, *J. Pharm. Sci.*, 1979, **68**, 1124–1127.
- A. B. Pinkerton, J.-M. Vernier, H. Schaffhauser, B. A. Rowe, U. C. Campbell, D. E. Rodriguez, D. S. Lorrain, C. S. Baccei, L. P. Daggett and L. J. Bristow, *J. Med. Chem.*, 2004, **47**, 4595–4599.
- V. Sedova and O. Shkurko, *Chem. Heterocycl. Compd.*, 2004, **40**, 194–202.
- X. Lang, X. Chen and J. Zhao, *Chem. Soc. Rev.*, 2014, **43**, 473–486.
- J. M. Narayanam and C. R. Stephenson, *Chem. Soc. Rev.*, 2011, **40**, 102–113.
- C. K. Prier, D. A. Rankic and D. W. MacMillan, *Chem. Rev.*, 2013, **113**, 5322–5363.

- 42 B. Bandgar and K. Shaikh, *Tetrahedron Lett.*, 2003, **44**, 1959–1961.
- 43 B. M. Trost, *Angew. Chem., Int. Ed.*, 1995, **34**, 259–281.
- 44 J. Breitenfeld, O. Vechorkin, C. m. Corminboeuf, R. Scopelliti and X. Hu, *Organometallics*, 2010, **29**, 3686–3689.
- 45 A. Ostroushko, M. Tonkushina, A. Safronov, S. Y. Men'shikov and V. Y. Karataev, *Russ. J. Org. Chem.*, 2009, **54**, 204–211.
- 46 X.-J. Kong, L.-S. Long, Z. Zheng, R.-B. Huang and L.-S. Zheng, *Acc. Chem. Res.*, 2009, **43**, 201–209.
- 47 E. Mizushima, K. Sato, T. Hayashi and M. Tanaka, *Angew. Chem.*, 2002, **114**, 4745–4747.
- 48 A. Leyva and A. Corma, *J. Org. Chem.*, 2009, **74**, 2067–2074.
- 49 P. Roembke, H. Schmidbaur, S. Cronje and H. Raubenheimer, *J. Mol. Catal. A: Chem.*, 2004, **212**, 35–42.
- 50 M. Tokunaga and Y. Wakatsuki, *Angew. Chem., Int. Ed.*, 1998, **37**, 2867–2869.
- 51 T. Suzuki, M. Tokunaga and Y. Wakatsuki, *Org. Lett.*, 2001, **3**, 735–737.
- 52 W. Baidossi, M. Lahav and J. Blum, *J. Org. Chem.*, 1997, **62**, 669–672.
- 53 N. Watfa, S. Floquet, E. Terazzi, W. Salomon, L. Guénée, K. L. Buchwalder, A. Hijazi, D. Naoufal, C. Piguet and E. Cadot, *Inorganics*, 2015, **3**, 246–266.
- 54 S. Garai, E. T. Haupt, H. Bögge, A. Merca and A. Müller, *Angew. Chem.*, 2012, **124**, 10680–10683.
- 55 I. Ghosh, R. S. Shaikh and B. König, *Angew. Chem., Int. Ed.*, 2017, **56**, 8544–8549.
- 56 W.-J. Xiao, Q.-Q. Zhou, Y.-Q. Zou and L.-Q. Lu, *Angew. Chem., Int. Ed.*, 2018, DOI: 10.1002/anie.201803102.
- 57 Z. D. Miller, B. J. Lee and T. P. Yoon, *Angew. Chem.*, 2017, **129**, 12053–12057.
- 58 Z. Zuo, D. T. Ahneman, L. Chu, J. A. Terrett, A. G. Doyle and D. W. MacMillan, *Science*, 2014, **345**, 437–440.
- 59 G. Bernardini, A. G. Wedd, C. Zhao and A. M. Bond, *Proc. Natl. Acad. Sci. U. S. A.*, 2012, **109**, 11552–11557.